Dynamic phase transition induced by active molecules in a supercooled liquid

Victor Teboul *

Laboratoire de Photonique d'Angers EA 4464, Université d'Angers, Physics Department, 2 Bd Lavoisier, 49045 Angers, France

(Received 21 February 2023; accepted 21 July 2023; published 10 August 2023)

The purpose of this work is to use active particles to investigate the effect of facilitation on supercooled liquids. To this end we examine the behavior of a model supercooled liquid that is doped with a mixture of active particles and slowed particles. To simulate the facilitation mechanism, the activated particles are subjected to a force that follows the mobility of their most mobile neighboring molecule, while the slowed particles experience a friction force. Upon activation, we observe a fluidization of the entire medium along with a significant increase in dynamic heterogeneity. This effect is reminiscent of the fluidization observed experimentally when introducing molecular motors into soft materials. Interestingly, when the characteristic time τ_μ, used to define the mobility in the facilitation mechanism, matches the physical time t^* that characterizes the spontaneous cooperativity of the material, we observe a phase transition accompanied by structural aggregation of the active molecules. This transition is characterized by a sharp increase in fluidization and dynamic heterogeneity.

DOI: 10.1103/PhysRevE.108.024605

I. INTRODUCTION

Media that contain particles capable of self-propulsion, such as molecular motors or nanomachines [1–19], are called actives. Active matter is retaining much attention by the scientific community due to its connection with biology and out-of-equilibrium statistical physics [20]. Active matter also provides a new route for studying the glass transition problem [21–30], due to its non equilibrium physical properties and potential origins. That line of research has already led to a number of interesting results [15,20,31–57]. It has been discovered that the glass transition persists in active matter, albeit at a different transition temperature. Under specific conditions, a dynamical slowing down appears upon activation, while in most cases fluidization is observed [32,51–57]. Notably, an interesting study [32] revealed a fluidization of the medium together with a tendency for active molecules to form clusters. Induced fluidization has also been reported experimentally [18,19,58–66] and through simulations when simple molecular motors [67–76] activate a soft material.

However, for supercooled liquids in their approach to the glass transition, the mobility replaces the velocity as a relevant parameter. This is due to the cage effect that erases the dependence of physical mechanisms on instantaneous velocity direction. Therefore, in this study, we pose the question of how using mobility rather than velocity inside the activation force definition affects the results.

Facilitation mechanisms have been proposed as the origin of the glass transition and the emergence of cooperative motions, namely dynamic heterogeneity. In that picture, at low temperatures when motion is scarce, the motion of a nearby molecule is needed to facilitate the motion of any molecule. Consequently, facilitation mechanisms promote cooperative motions. The entanglement of trajectories induced by facilitation coupled with the increased scarcity of excitations at low temperature were also suggested to induce the glass transition [77].

In our study, we create a facilitation mechanism using a small number of periodically activated molecules. Each of these molecules is activated by a propulsive force of constant magnitude, aligned with the mobility of its most mobile neighbor. This approach allows us to directly examine the effects of facilitation mechanisms in a supercooled medium. We find that a phase transition results from these activation laws, with a large increase of dynamical heterogeneity and a large modification of transport coefficients. The facilitation induces an important fluidization of the medium when the mobility timescale τ_μ employed in the activation mechanism reaches a critical value that increases as the temperature decreases.

II. CALCULATION

A. Model

The purpose of our study is to test an out-of-equilibrium model that mimics the behavior of supercooled liquids. Traditionally, simulations create active media by applying a propulsive force to molecules, usually aligned with their velocities. Sometimes, an interaction that induces correlated displacements of molecules is introduced, to simulate collective motions resembling those observed in living organisms. In this work we investigate the effect of forces that better capture the physics of supercooled liquids. Thus, our propulsive force follows the mobility of molecules rather than their velocity, and correlation in velocities are replaced by correlations in mobilities of molecules. We expect that activating our medium with relevant parameters will increase (or decrease) the thermal cooperativity of the medium in its approach to the glass transition, resulting in a modification of the transition and physical properties of the medium that we will study.

We employ out-of-equilibrium molecular dynamic simulations [78–81] to obtain results that are more easily

*victor.teboul@univ-angers.fr

comprehensible and comparable to previous studies on molecular motors [64,66,82–85], particularly regarding fluidization phenomena observed experimentally and theoretically [58–65] when molecular motors are dispersed within soft materials.

We use dumbbell molecules constituted of two rigidly bonded atoms ($i = 1, 2$) at the fixed interatomic distance $l = 1.73$ Å. These atoms interact with atoms of other molecules with the following Lennard-Jones potentials:

$$V_{ij} = 4\epsilon_{ij}((\sigma_{ij}/r)^{12} - (\sigma_{ij}/r)^{6}), \tag{1}$$

with the parameters [86] $\epsilon_{11} = \epsilon_{12} = 0.5$ KJ/mol, $\epsilon_{22} = 0.4$ KJ/mol, $\sigma_{11} = \sigma_{12} = 3.45$ Å, $\sigma_{22} = 3.28$ Å. The mass of the molecule is $m = 80$ g/mole (2 atoms with a mass of 40 g/mole each). The length of the molecule is therefore $l_m = 5.09$ Å and its width $L_m = 3.37$ Å. Our cubic simulation boxes contain 1000 molecules and are 32.49 Å large, or 2000 molecules and are 40.9 Å large.

The system is maintained out of equilibrium by the presence of active molecules releasing energy into it and damped molecules absorbing energy. As a result our system with an adequate choice of the damping parameter while out of equilibrium is approximately in a steady state, the damped molecules removing the energy released in our system by the activated molecules. Nonetheless, we include a small thermostat [87] to avoid any possible energy drift.

In our calculations, 10% of the medium molecules are periodically damped for 10 ps within a 40 ps time interval. Simultaneously, another 10% of the medium molecules are periodically activated (for 10 ps within a 40 ps time interval) in a direction parallel to the mobility of their most mobile neighbors. Therefore, at time t, 2.5% of the molecules are damped and 2.5% are accelerated, while the other 95% molecules experience only intermolecular interactions.

We define the mobility $\boldsymbol{\mu}_i(t)$ of a molecule i as

$$\boldsymbol{\mu}_i(t) = \mathbf{r}_i(t + \tau_\mu) - \mathbf{r}_i(t), \tag{2}$$

where τ_μ represents the characteristic time of the mobility. By tuning τ_μ we expect to find a significant response of our liquid when τ_μ will match an important characteristic time scale of the physics of our medium.

Activated molecules are periodically subject to a force $\mathbf{f}_i^a$ of constant intensity f_0, acting during 10 ps within a time interval $T = 40$ ps. The forces $\mathbf{f}_i^a$ are limited to a set of molecules called active, and begin with a different random time origin for each molecule, following the law

$$\mathbf{f}_i^a(\tau_\mu, t) = f_0\theta_{i,T,\Delta T}(t)\mathbf{u}_{i,\mu_{\max}}^{\text{neighbor}}(t, \tau_\mu). \tag{3}$$

Here $\theta_{i,T,\Delta T}(t)$ is a periodic heaviside function, equal to 1 during $\Delta T = 10$ ps and zero otherwise with a period $T = 40$ ps. $f_0 = 6.02\ 10^{-14}N$ is the constant intensity of the force when activated.

$$\mathbf{u}_{i,\mu_{\max}}^{\text{neighbor}}(t, \tau_\mu) = \boldsymbol{\mu}_j(t, \tau_\mu)/|\mu_j(t, \tau_\mu)| \tag{4}$$

is the unit vector of the mobility of the most mobile neighbor j of molecule i (see Fig. 1 for description).

The damped molecules are subject to a force $\mathbf{f}_i^d$ proportional to their velocity

$$\mathbf{f}_i^d(t) = -\alpha.f_0\theta_{i,T,\Delta T}(t)\mathbf{v}_i(t)/\bar{v}, \tag{5}$$

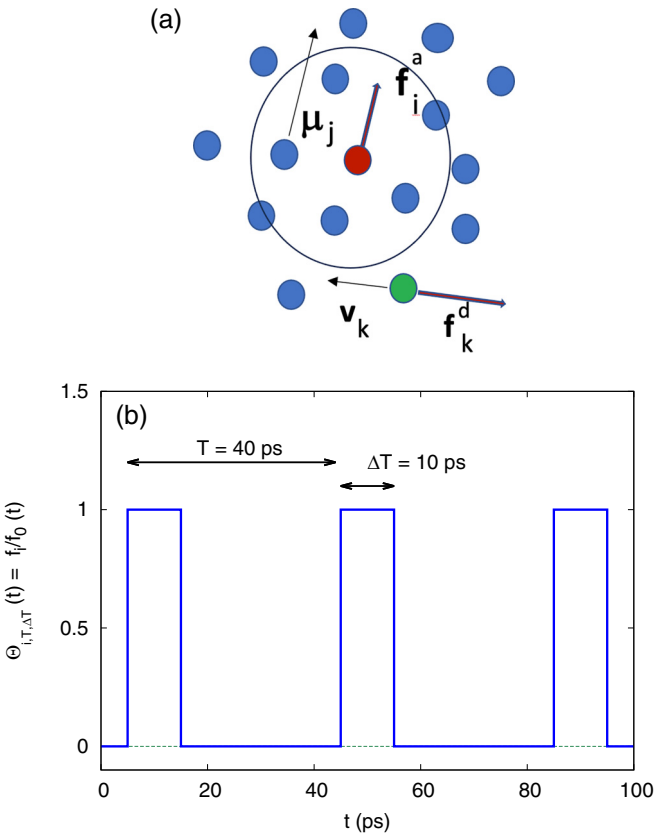

FIG. 1. (a) Description of the facilitation mechanism used for the 2.5% active molecules at an instant t. During its activation period a force $\mathbf{f}_i^a$ of constant magnitude is applied to active molecule i (red) in a direction parallel to the mobility $\boldsymbol{\mu}_j(t)$ of the most mobile surrounding j molecule. Thus $\mathbf{f}_i^a(\tau_\mu, t) = f_0\theta_{i,T,\Delta T}(t)\boldsymbol{\mu}_j(t, \tau_\mu)/|\mu_j(t, \tau_\mu)|$, where j is the most mobile molecule surrounding i and f_0 is a constant. An equal number of molecules k are periodically damped (green). The force acts on atoms 1 of the dumbbells only. Each molecule is displayed as one bead (atoms 1 only) for clarity of the Figure. The circle shows the first neighbors shell. (b) Description of the periodic evolution of the force on an active molecule i. The time origin of the periodic activation or damping is chosen randomly for each molecule.

where $\bar{v} = \sqrt{\frac{8RT}{\pi m}}$ is the average velocity modulus, $m = 80$ g/mol is the molar mass of a molecule and the temperature is $T = 500$ K. $\alpha = 9.1$ is a coefficient chosen so that the energy absorbed by damped molecules approximately compensate in our system the energy released by active molecules. Our medium is a minimal model liquid [86] constituted of dumbbell diatomic molecules (each atom being of the same mass $m_0 = 40\text{g}/N_A$) chosen to hinder crystallization [88,89] and accelerate the simulations. However, due to the use of Lennard-Jones potentials only, the results can be easily shifted to model although approximately a large number of real viscous liquids.

B. Statistical functions

In this study, we examine the modification of key characteristics in supercooled liquids, such as the presence of dynamic heterogeneity, diffusion properties, and the α relaxation time related to the viscosity of the medium. Let us

now define the statistical functions utilized for this purpose. The most adequate function to measure the strength of the dynamic heterogeneity [90–93] is the dynamic susceptibility χ_4 defined as [90]

$$\chi_4(a,t) = \frac{\beta V}{N^2}(\langle C_a(t)^2\rangle - \langle C_a(t)\rangle^2), \tag{6}$$

with

$$C_a(t) = \sum_{i=1}^{N} w_a(|\mathbf{r}_i(t) - \mathbf{r}_i(0)|). \tag{7}$$

In these equations, V denotes the volume of the simulation box, N denotes the number of molecules in the box, and $\beta = (k_B T)^{-1}$. Also, the symbol w_a stands for a discrete mobility window function $w_a(r)$, taking the values $w_a(r) = 1$ for $r < a$ and zero otherwise. We use the value $a_0 = 1$ Å below the transition [94] or for the nonactivated liquid and $a_1 = 2$ Å above the transition, values that in these conditions maximize $\chi_4(a,t)$. The non-Gaussian parameter (NGP) $\alpha_2(t)$ is also often used as a measure of dynamic heterogeneity

$$\alpha_2(t) = \frac{d}{d+2}\frac{\langle r^4(t)\rangle}{\langle r^2(t)\rangle^2} - 1, \tag{8}$$

where $d = 3$ is the system dimension. It has the advantage of being simple to interpret and to have a characteristic time t^* directly related to the physics of the liquid. We define t^* as the time for which $\alpha_2(t)$ reaches its maximum. Due to the definition of $\alpha_2(t)$, in most supercooled liquids t^* is the characteristic time of cooperative motions (DHs). Another function of large interest in glass-transition related phenomena is the intermediate scattering function $F_S(Q,t)$ that represents the autocorrelation of the density fluctuations at the wave vector Q. This function gives information on the structural relaxation of the material. We define $F_S(Q,t)$ by the relation

$$F_S(Q,t) = \frac{1}{NN_{t_0}} Re\left(\sum_{i,t_0} e^{i\mathbf{Q}.(\mathbf{r_i(t+t_0)}-\mathbf{r_i(t_0)})}\right). \tag{9}$$

For physical reasons, Q is chosen as the wave vector (here $Q_0 = 2.25$ Å^{-1}) corresponding to the maximum of the structure factor $S(Q)$. $F_S(Q_0,t)$ then allows us to calculate the α relaxation time τ_α of the medium from the equation

$$F_S(Q_0,\tau_\alpha) = e^{-1}. \tag{10}$$

Finally, the diffusion coefficient D is obtained from the long-time limit of the mean square displacement $\langle r^2(t)\rangle$:

$$\langle r^2(t)\rangle = \frac{1}{NN_{t_0}}\sum_{i,t_0}(\mathbf{r}_i(t+t_0) - \mathbf{r}_i(t_0))^2 \tag{11}$$

and

$$\lim_{t\to\infty}\langle r^2(t)\rangle = 2dDt. \tag{12}$$

C. Size effects

As phase transition are usually associated with diverging correlation lengths, large size effects are expected to take place around the transition as a signature of a phase transition. The large increase of cooperative effects above the transition

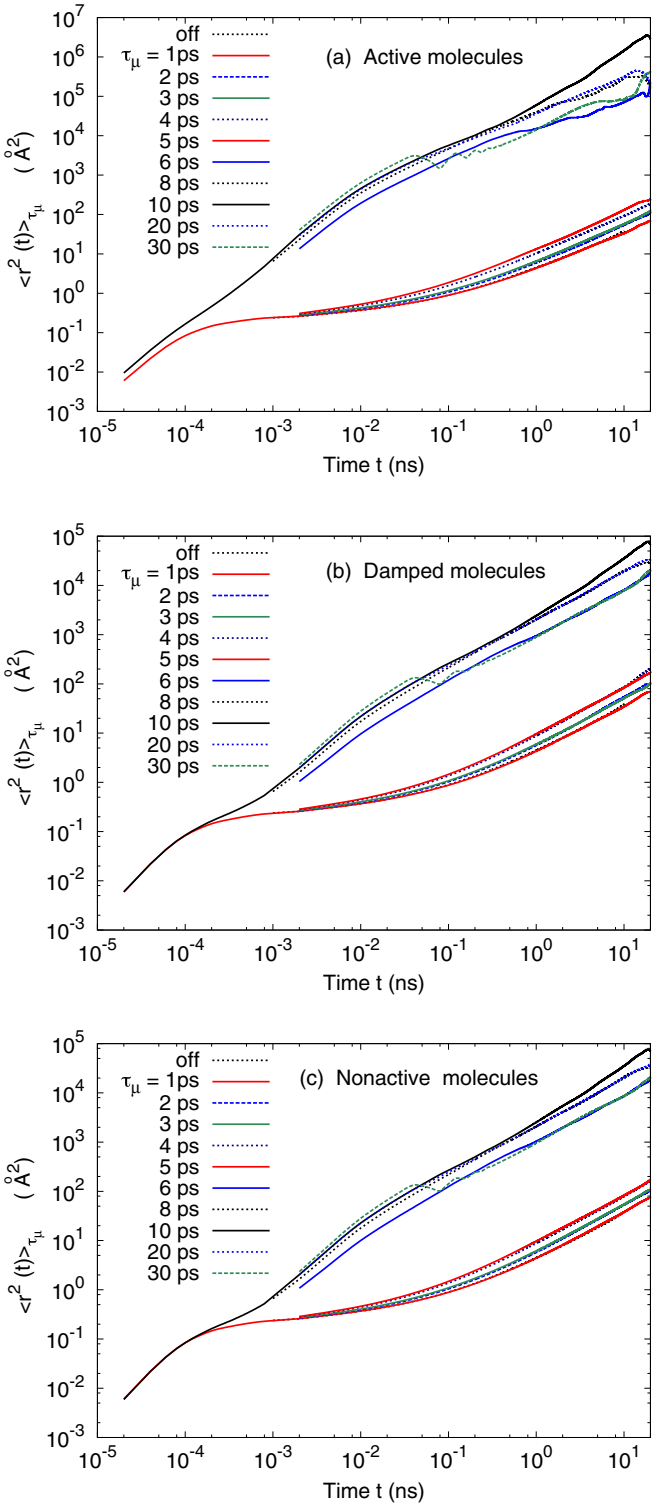

FIG. 2. Mean square displacement $\langle r^2(t)\rangle$ of (a) the 10 percent intermittently active molecules, (b) the 10 percent intermittently damped molecules, (c) the 80 percent medium molecules moving freely. τ_μ is the characteristic time chosen for the mobility definition acting in the activation force (see the calculation section for details). Active molecules are activated during 1/4 of a time period $T = 40$ ps that begins randomly for each active molecule. Consequently there are only an average of 2.5 percent of molecules active at a given time t and similarly 2.5 percent of damped molecules.

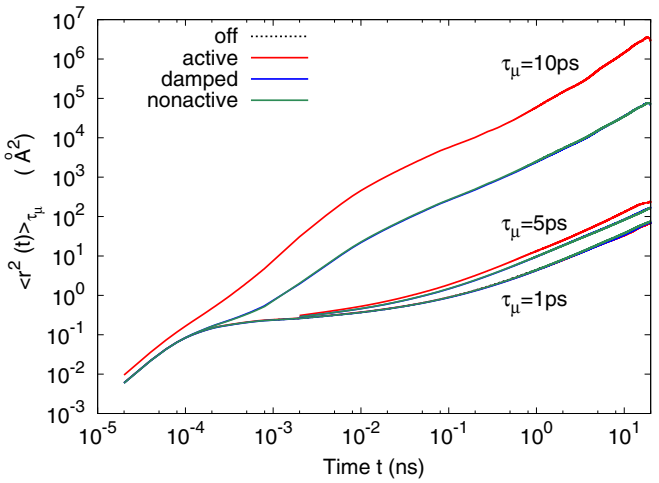

FIG. 3. Mean square displacement $\langle r^2(t)\rangle$ for various values of τ_μ (the characteristic time chosen for the mobility definition acting in the activation force). There is not much difference between active and damped molecules below the transition, while above the transition active molecules are more mobile due to their aggregation.

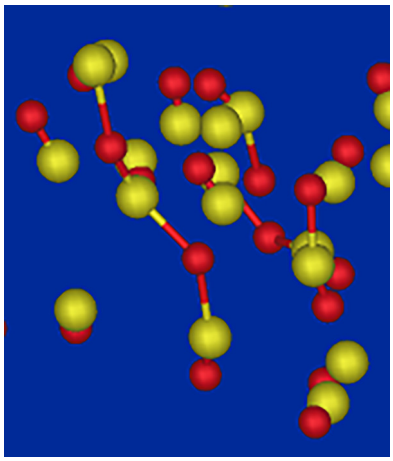

FIG. 5. Motion of active molecules on the time scale τ_μ of their chosen mobility, above the transition ($\tau_\mu = 8$ ps). Only the larger atom of the molecule is represented. The location of the atom at time t_0 is plotted in red (small), and at time $t_0 + \tau_\mu$ in yellow (large). We observe strings of mobile molecules in their process to aggregation.

also may lead to size effects. It is therefore important to test our results for size effects. To this aim we varied the simulation boxes sizes from $N = 500$ molecules ($l_x = 25.8$ Å) to $N = 4000$ molecules ($l_x = 51.5$ Å). We didn't find significant size effects below the transition for $N > 600$ molecules, while above the transition size effects are significant and disappear totally for $N \geqslant 2000$ molecules only [95]. Results show that the transition is stronger when the box is made larger (that is, the diffusion and dynamic heterogeneities increase above the transition when increasing the box size).

III. RESULTS AND DISCUSSION

A. Medium fluidization

When active and damped molecules are together introduced inside the medium, we observe its fluidization. This fluidization increases with the choice of mobility's characteristic time τ_μ. Figures 2 and 3 illustrate that behavior displaying the evolution of the mean square displacements $\langle r^2(t)\rangle_{\tau_\mu}$ with τ_μ of active, inactive, and damped molecules. A sharp increase appears at the critical value $\tau_\mu^c = 5.6$ ps [94]. For the same value of $\tau_\mu \geqslant \tau_\mu^c$ we observe a sharp structural aggregation of mobile molecules (see Fig. 4) showing a dynamic phase transition associated with the mobility [94]. We thus explain the sharp increase of the displacements as due to the structural aggregation of active molecules that facilitates their motion.

Figure 2 shows that not only the active molecules undergo a transition in mobility, but also the large set of nonactive molecules and even the damped molecules. In Fig. 3 we compare the MSD of the different set of molecules

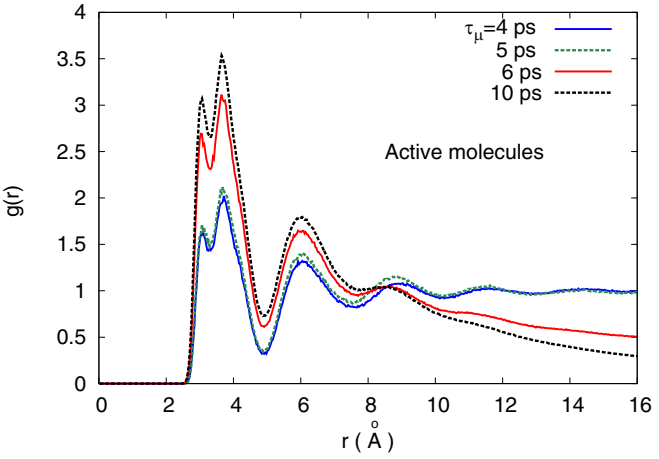

FIG. 4. Radial distribution function $g(r)_{\text{active}-\text{active}}$ between the 10 percent intermittently active molecules for different values of the parameter τ_μ. We observe the aggregation of the active molecules at the phase transition, that is when $\tau_\mu \geqslant \tau_\mu^c = 5.6$ ps.

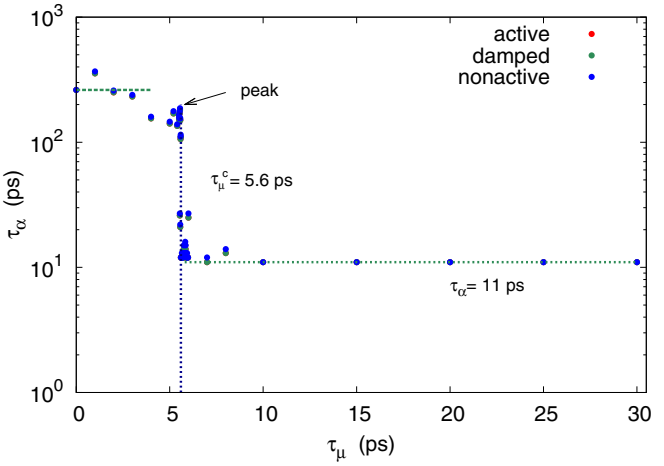

FIG. 6. Alpha relaxation time τ_α as a function of τ_μ. τ_α is here obtained from the relation $F_s(Q_0, \tau_\alpha) = e^{-1}$ where $Q_0 = 2.25$ Å^{-1}. The first point ($\tau_\mu = 0$) and the green line correspond to the nonactivated liquid value.

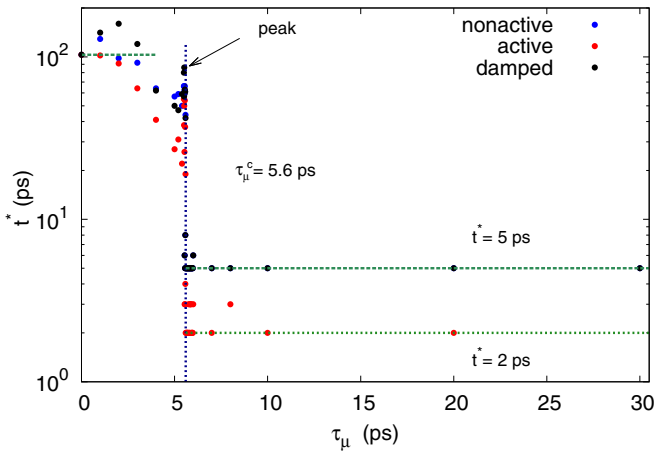

FIG. 7. Non-Gaussian parameter $\alpha_2(t)$ characteristic time t^* versus τ_μ parameter. $\tau_\mu = 0$ and the green line correspond to the nonactivated liquid.

(actives, inactives, and damped) for different values of the characteristic time τ_μ. For short values of the characteristic time ($\tau_\mu = 1$ ps on the plot), the activation does not affect the MSDs, then as the characteristic time increases, the active molecules MSD split slightly from the two other curves. Eventually, when the characteristic time reaches the transition value, the active molecules curve separates itself importantly from the two other curves and we observe a factor larger than 10 for $\tau_\mu = 10$ ps, while the damped and nonactive sets of particles lead unexpectedly to the exact same MSDs.

We will find this behavior, that is a slow drift from the nonactive liquid values below the transition followed by a large evolution at the transition, for the whole set of statistical parameters studied. To show that effect, a small line emphasizes the nonactive liquid values in most figures. This behavior suggests that τ_μ has to reach a critical value, linked to the physics of the supercooled liquid, for the system to respond to the active molecules stimulation.

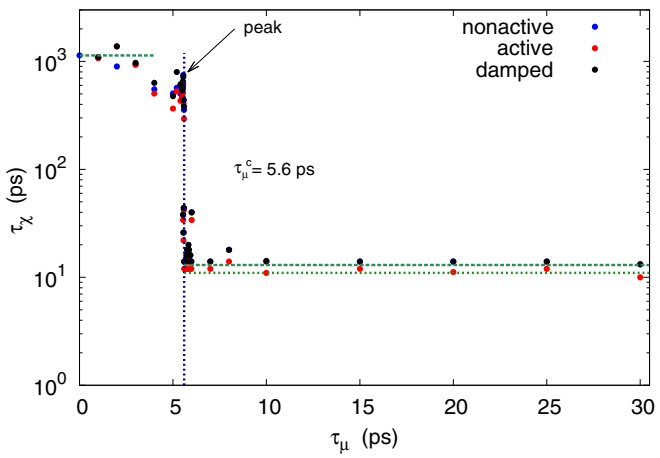

FIG. 8. Characteristic time τ_χ of our dynamic susceptibility, defined as the time for which $\chi_4(a_1, t)$ reaches its maximum value, versus τ_μ. $a_1 = 2$ Å (the optimum above the transition).

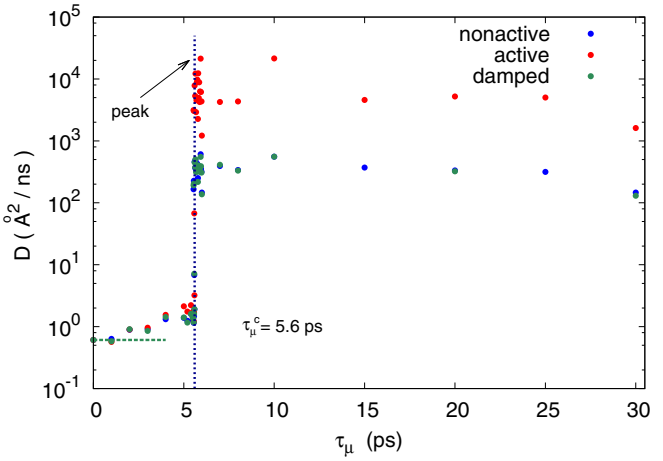

FIG. 9. Diffusion coefficient D versus τ_μ, where τ_μ is the characteristic time chosen for the mobility definition acting in the activation force.

B. Aggregation of active molecules

The structure of the different sets of molecules (i.e., active, damped, and normal) is similar below the transition [94], i.e., for $\tau_\mu \leqslant \tau_\mu^c$ to the structure without activation. Then at the transition and above the transition, the active molecules aggregate as shown in Figs. 4 and 5, while the other sets of molecules do not (not shown). We interpret this aggregation of the active molecules as the main cause of the acceleration of the liquid dynamics. In that picture, because the active molecules are the most mobile, their aggregation facilitates their motion due to the decrease of their surrounding viscosity.

The characteristics of an aggregation are observed in Fig. 4 for $\tau_\mu = \tau_\mu^c$ and 10 ps as the first two peaks that represent the density probability to have active molecules as first and second neighbors increase while the density probability at larger distances decrease. In contrast, below the transition we observe a radial distribution function very typical for a liquid and that is identical to the RDF of the liquid without activated molecules. Below the transition, for $r > 10$ Å the radial distribution $g(r) \approx 1$ showing the homogeneity of the medium after the third neighbor correlation, while the depletion above the transition shows that the active molecules have migrated to shorter distances.

C. Characteristic times evolution

We observe a transition at $\tau_\mu^c = 5.6$ ps for the two characteristic times studied, the α relaxation time τ_α (Fig. 6) characterizing the liquid local dynamics, and the characteristic time t^* that characterizes the heterogeneous dynamics (Fig. 7), and the characteristic time τ_χ of the susceptibility in Fig. 8.

Above the transition [94], we find $\tau_\alpha \approx 2\tau_\mu^c$ and $t^* \approx \tau_\mu^c$. If one expects that $\tau_\alpha > t^*$ as τ_α corresponds to the complete relaxation of the medium, while t^* corresponds to the very beginning of the cage escaping process that leads eventually to the relaxation, the fact that $t^* \approx \tau_\mu^c$ is however of particular interest, as it suggests that τ_μ interacts with the medium's cooperativity.

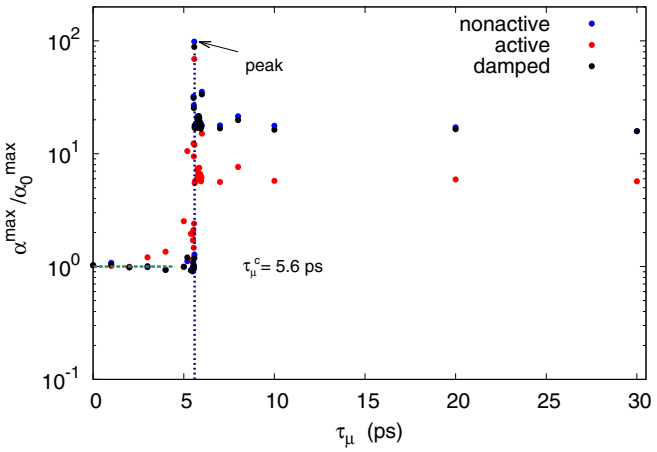

FIG. 10. Non-Gaussian parameter $\alpha_2(t)$ normalized maximum value versus τ_μ parameter. τ_μ is the characteristic time chosen for the mobility definition acting in the activation force. The arrow shows the peak of the dynamical heterogeneity at the transition.

The same transition appears for the diffusion coefficient D (Fig. 9) and as a result to the associated characteristic time $\tau_D = \frac{b^2}{D}$ where we define the characteristic length b as the average distance necessary to get outside the cage created by the surrounding molecules.

When τ_μ increases, the characteristic times first decrease continuously then drop to a constant value as $\tau_\mu^c = 5.6$ ps is reached. Notice that on the transition we observe for the whole set of parameters a small peak (Figs. 6–12) corresponding to an increase of the characteristic times (t^* and τ_α), while the diffusion coefficient unexpectedly increases (τ_D decreases). The origin of this slowing down located at the transition, just before the large fluidization, appears related to a cooperativity increase. We observe indeed a similar peak for the non-Gaussian parameter (Fig. 10) and for the deviation from the Stokes-Einstein law (Fig. 11) showing that the dynamic is highly cooperative at that point, as expected for a phase transition [96–98]. The dynamic susceptibility for nonactive

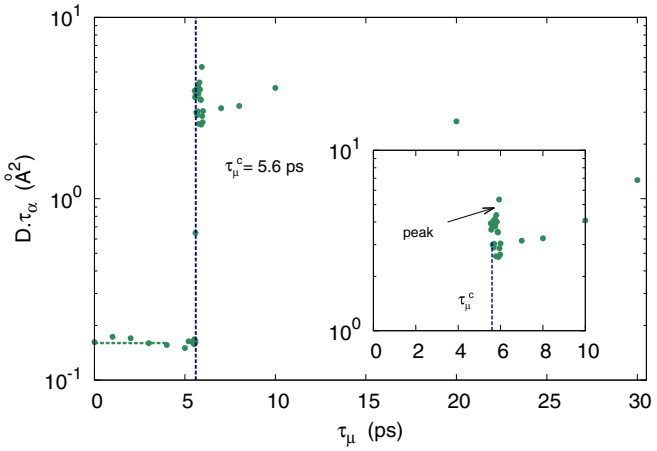

FIG. 11. Breaking of the Stokes-Einstein relation versus τ_μ parameter. The first point ($\tau_\mu = 0$) and the green line correspond to the nonactivated liquid value.

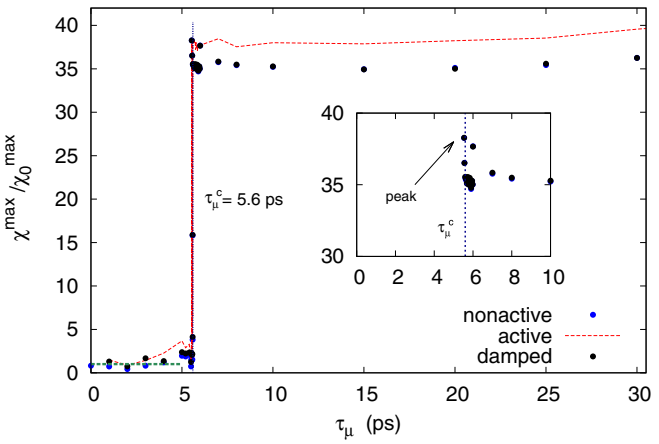

FIG. 12. Dynamic susceptibility maximum value $\chi_4(a_1,t)^{\max}$ normalized by the maximum value in the nonactive liquid $\chi_4(a_0,t)_0^{\max}$ versus τ_μ. For clarity, we have chosen here $a_1 = 2$ Å (the optimum above the transition) and $a_0 = 1$ Å (the optimum value without activation and below the transition) for the whole set of points.

molecules displays also a small peak that reaches the active value in Fig. 12.

D. Increase of dynamical heterogeneity upon activation

Dynamical heterogeneity (DH) [90–93], are together with a dramatic increase of the medium's viscosity, a hallmark of supercooled liquids in their approach to the glass transition. They are characterized by the spontaneous aggregation of most mobile molecules on a characteristic time t^* and stringlike cooperative motions of these molecules (Fig. 5), on the same characteristic time. As cooperative mechanisms are expected with a rising associated susceptibility in any phase transition, these cooperative mechanisms have long been suspected to be the fingerprint of a thermodynamic phase transition explaining the glass transition. Also, the DHs are a crucial element in facilitation theories [77,99–103].

Below the phase transition [94], i.e., for $\tau_\mu < \tau_\mu^c$ after a small decrease of the dynamic susceptibility for $\tau_\mu = 1$ to 2 ps we observe in Fig. 13(a) a significant increase of the susceptibility with τ_μ leading to a value equal to twice the thermal susceptibility $\chi_4(a_0,t)_0^{\max}$ for $\tau_\mu = \tau_\mu^c$. We also observe a small decrease of the susceptibility characteristic time. The maximum value of the susceptibility is shifted to shorter times, i.e., τ_χ that maximizes $\chi_4(a,t)$ decreases. Figure 13 shows that τ_χ decreases from 250 ps without activation to 100 ps for $\tau_\mu = 5$ ps just before the transition. Above the transition, i.e., for $\tau_\mu > \tau_\mu^c$ [Fig. 13(b)], the susceptibility behavior changes drastically and we observe a huge increase of the susceptibility, leading to a value 25 times larger than the thermal susceptibility. The susceptibility characteristic time also undergoes a strong evolution above the transition, decreasing from 250 ps for the thermal susceptibility to values around 10 ps.

Figure 12 resumes that behavior showing an abrupt transition on the susceptibility for $\tau_\mu \approx \tau_\mu^c$. This Figure compares well with Figs. 9 and 6 displaying a similar abrupt transition

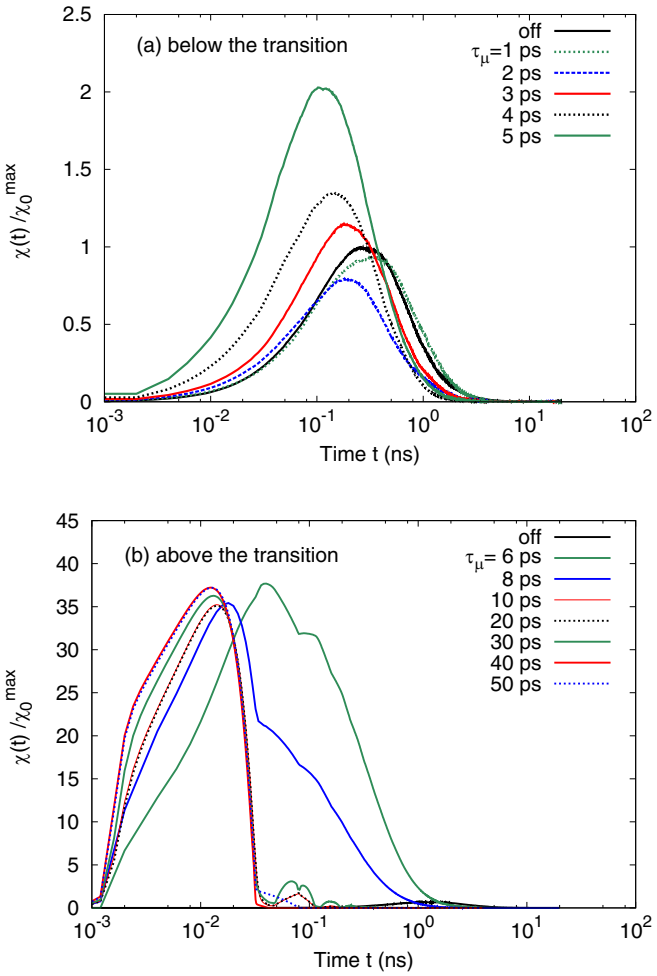

FIG. 13. Dynamic susceptibility $\chi_4(a_\alpha, t)$ normalized by its maximum value in the nonactive liquid $\chi_4(a_\alpha, t)_0^{\max}$ versus τ_μ parameter. $\chi_4(a_\alpha, t)/\chi_4(a_\alpha, t)_0^{\max}$ is shown for the 80 percent medium molecules moving freely. (a) Below the transition, (b) above the transition. The length parameter a_α is chosen to optimize the susceptibility [Eqs. (5) and (6)]. (a) $a_\alpha = a_0 = 1$ Å and (b) $a_\alpha = a_1 = 2$ Å, which correspond to the optimum respectively below and above the transition, for the nonactivated liquid. τ_μ is the characteristic time chosen for the mobility definition acting in the activation force. Note that in the vicinity of the transition the susceptibility is much larger. The plots correspond to the nonactivated liquid. We do not display the active and damped molecules subsets that lead to quite similar curves.

for the diffusion coefficient and the alpha relaxation time for the same value of τ_μ.

We therefore observe a phase transition controlled by the mobility time parameter τ_μ showing a large increase of the cooperative behavior (DH) associated to the fluidization of the medium. The association of an increase of dynamic heterogeneity with a decrease of the viscosity, while quite unusual, has been observed in fluidization processes by activation of materials with molecular motors.

As a tentative picture, in these activated systems the activation induces the dynamic heterogeneity, cooperative motions that in turn induce the fluidization (i.e., a decrease of the viscosity and an increase of the diffusion coefficient).

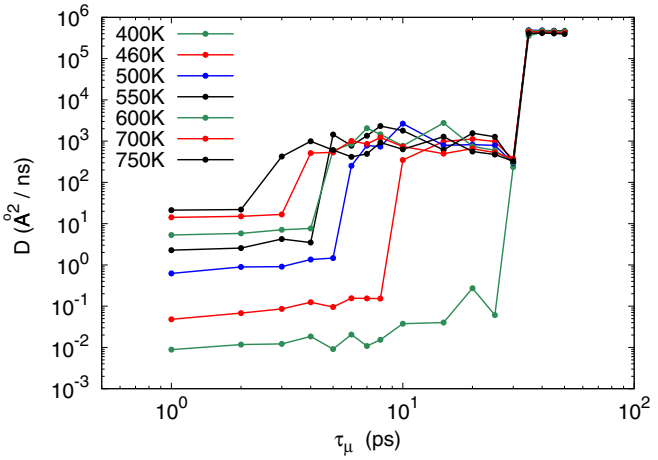

FIG. 14. Diffusion coefficient D averaged on the whole set of molecules versus τ_μ parameter, at different temperatures. As the temperature drops the transition is shifted to larger times τ_μ^c. τ_μ^c therefore follows the nonactivated liquid timescales temperature evolution.

What is the difference in the cooperative behavior of active, nonactive, and damped molecules subsets? We found that below the transition, the maximum difference is observed for $\tau_\mu = 5$ ps in the vicinity of the transition. We find the normalized susceptibility to be larger for active molecules than damped molecules and larger for damped molecules than nonactive ones. However the difference is relatively small. While above the transition the difference is even smaller in relative values. Therefore, the differences observed for active, nonactive, and damped molecules for the susceptibility are small, showing that the whole medium's cooperativity is affected by active molecules motion.

The large increase of the DHs at the transition observed with the dynamic susceptibility are confirmed with other measures of the dynamic heterogeneity, as the non-Gaussian parameter (Figs. 10 and 7) and the breaking of the Stokes-Einstein law (Fig. 11). To summarize, we observe for all the statistical functions considered [$\alpha_2(t)$, $\chi_4(t)$, $D.\tau_\alpha$, D, and τ_α] an important reaction of the system when the mobility used for the activation of molecules corresponds to the physical mobility of the medium.

E. Evolution of the transition with temperature

When the liquid is not activated, a drop in temperature leads to an increase of the characteristic timescales as expected for a supercooled liquid [86]. Results show (see Fig. 14) that the transition follows the same trend. τ_μ^c increases when the temperature drops suggesting a direct link between the liquid characteristic timescales and the characteristic time of the transition [95].

IV. INTERPRETATION

Active molecules are expected to induce higher mobility in their surroundings, while damped molecules impede motion in their vicinity. In supercooled liquids, this effect is amplified due to the rise of cooperativity. However, in our system additional phenomena come into play. Since active

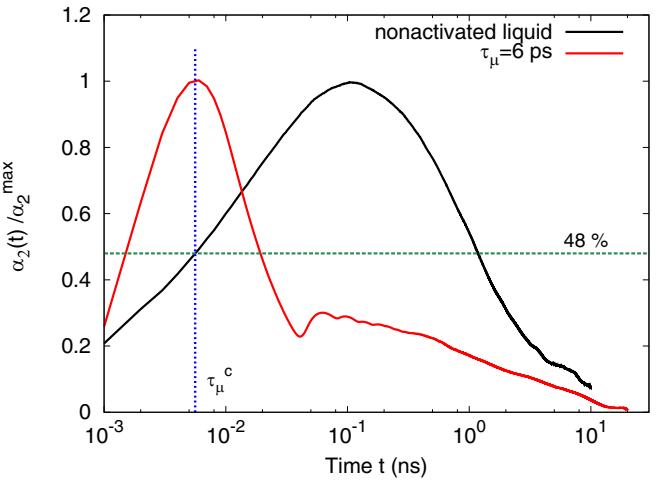

FIG. 15. Non-Gaussian parameter $\alpha_2(t)$ normalized by its maximum value, versus time for the nonactivated liquid (black) and for the activated liquid above the transition (red). The nonactivated liquid non-Gaussian parameter reaches approximately half its maximum value for $t = \tau_\mu^c$. We also observe that the non-Gaussian parameter of the liquid above the transition has been shifted to shorter times by the activation so that its maximum is around τ_μ^c.

molecules are generally more mobile, if an active molecule is close to another one, their mobilities will be after a few time steps approximately in the same directions due to the force definition. Consequently, these active molecules have a probability of remaining in proximity to each other, due to similar mobilities resulting in similar displacements. Depending on the lifetime of these clusters it can result in the aggregation of active molecules and a phase transition accompanied with fluidization of the medium. However for the transition to occur, the force has to be in the direction of a physically relevant mobility, leading to a threshold for $\tau_\mu \approx t^*$.

If we found actually $\tau_\mu^c \approx t^*$, the characteristic time of cooperative motions t^* in that relation is the characteristic time above the transition [94] which is significantly smaller than below the transition. However, as shown in Fig. 15 the non-Gaussian parameter (that measures cooperativity) of the nonactivated liquid (therefore below the transition) reaches approximately half its maximum value for $t = \tau_\mu^c = 5.6$ ps. τ_μ^c also corresponds to the physically important plateau time regime of the nonactivated liquid (see Fig. 2). Around that time value the activation mobility therefore begins to be significantly connected to the mobility of spontaneous cooperative motions of the supercooled liquid so that it affects significantly the dynamics of the system. Then, as the medium fluidization takes place, the characteristic times of the system decrease, leading to the decrease of the characteristic time of cooperative motions (t^*) which eventually reaches approximately τ_μ^c (Figs. 7 and 15).

V. CONCLUSION

The aim of our study was to investigate facilitation mechanisms in supercooled liquids approaching the glass transition by using activated particles. We achieved this by introducing a facilitation mechanism through periodic activation of a small fraction (2.5%) of the molecules, and damping of an equal number of molecules. The activation involved applying a constant propulsive force parallel to the mobility of the most mobile neighbor. We observed that the introduced facilitation mechanism led to a dynamic phase transition in the entire liquid when the characteristic time used in defining mobility reached a critical value τ_μ^c. This transition was characterized by the aggregation of active molecules, a significant increase in dynamic susceptibility and a decrease in characteristic and relaxation times indicating fluidization of the medium. Once the fluidization occurred, the characteristic time of dynamic heterogeneity (t^*) matched the critical value τ_μ^c suggesting a connection between the natural cooperativity of the medium and the artificial facilitation by active molecules. In summary, our study revealed the occurrence of a phase transition resulting from our activation laws, accompanied by a substantial increase in dynamical heterogeneity and significant modifications in transport coefficients. The facilitation mechanism induced pronounced fluidization of the medium when the mobility timescale τ_μ reached a critical value which increased as the temperature decreased.

There are no conflicts of interest to declare.

[1] I. Aprahamian, ACS Cent. Sci. **6**, 347 (2020).
[2] J. Wang, *Nanomachines: Fundamentals and Applications*, (Wiley, Weinheim, 2013).
[3] A. P. Davis, Nature (London) **401**, 120 (1999).
[4] J. P. Sauvage, *Molecular Machines and Motors* (Springer, Berlin, 2001).
[5] J. R. Howse, R. A. L. Jones, A. J. Ryan, T. Gough, R. Vafabakhsh, and R. Golestanian, Phys. Rev. Lett. **99**, 048102 (2007).
[6] H. Karani, G. E. Pradillo, and P. M. Vlahovska, Phys. Rev. Lett. **123**, 208002 (2019).
[7] F. Novotny and M. Pumera, Sci. Rep. **9**, 13222 (2019).
[8] X. Arque, A. Romero-Rivera, F. Feixas, T. Patino, S. Osuna, and S. Sanchez, Nat. Commun. **10**, 2826 (2019).
[9] A. M. Brooks, M. Tasinkevych, S. Sabrina, D. Velegol, A. Sen, and K. J. M. Bishop, Nat. Commun. **10**, 495 (2019).
[10] P. Pietzonka, E. Fodor, C. Lohrmann, M. E. Cates, and U. Seifert, Phys. Rev. X **9**, 041032 (2019).
[11] C. Calero, J. Garcia-Torres, A. Ortiz-Ambriz, F. Sagues, I. Pagonabarraga, and P. Tierno, Nanoscale **11**, 18723 (2019).
[12] C. F. E. Schroer and A. Heuer, Phys. Rev. Lett. **110**, 067801 (2013).
[13] V. Teboul and S. Ciobotarescu, Phys. Chem. Chem. Phys. **23**, 8836 (2021).
[14] G. Rajonson, D. Poulet, M. Bruneau, and V. Teboul, J. Chem. Phys. **152**, 024503 (2020).
[15] V. Teboul and G. Rajonson, J. Chem. Phys. **150**, 144502 (2019).

[16] V. Teboul and G. Rajonson, Phys. Chem. Chem. Phys. **21**, 2472 (2019).
[17] G. Rajonson, S. Ciobotarescu, and V. Teboul, Phys. Chem. Chem. Phys. **20**, 10077 (2018).
[18] S. Ciobotarescu, S. Bechelli, G. Rajonson, S. Migirditch, B. Hester, N. Hurduc, and V. Teboul, Phys. Rev. E **96**, 062614 (2017).
[19] G. Delhaye, F. Mercier, and V. Teboul, Phys. Fluids **33**, 122001 (2021).
[20] O. Dauchot and H. Lowen, J. Chem. Phys. **151**, 114901 (2019).
[21] K. Binder and W. Kob, *Glassy Materials and Disordered Solids* (World Scientific, Singapore, 2011).
[22] P. G. Debenedetti, *Metastable Liquids* (Princeton University Press, Princeton, 1996).
[23] P. G. Wolynes and V. Lubchenko, *Structural Glasses and Supercooled Liquids* (Wiley, Hoboken, 2012).
[24] P. W. Anderson, Science **267**, 1610 (1995).
[25] C. A. Angell, Science **267**, 1924 (1995).
[26] F. Ritort and P. Sollich, Adv. Phys. **52**, 219 (2003).
[27] G. H. Fredrickson and H. C. Andersen, Phys. Rev. Lett. **53**, 1244 (1984).
[28] J. Jackle and S. Eisinger, Z. Phys. B **84**, 115 (1991).
[29] W. Kob and H. C. Andersen, Phys. Rev. E **48**, 4364 (1993).
[30] V. Teboul, J. Chem. Phys. **141**, 194501 (2014).
[31] C. Bechinger, R. Di Leonardo, H. Lowen, C. Reichhardt, G. Volpe, and G. Volpe, Rev. Mod. Phys. **88**, 045006 (2016).
[32] R. Mandal, P. J. Bhuyan, M. Rao, and C. Dasgupta, Soft Matter **12**, 6268 (2016).
[33] R. Mandal, P. J. Bhuyan, P. Chaudhuri, M. Rao, and C. Dasgupta, Phys. Rev. E **96**, 042605 (2017).
[34] R. Mandal, P. J. Bhuyan, P. Chaudhuri, C. Dasgupta, and M. Rao, Nat. Commun. **11**, 2581 (2020).
[35] A. P. Solon, J. Stenhammar, R. Wittkowski, M. Kardar, Y. Kafri, M. E. Cates, and J. Tailleur, Phys. Rev. Lett. **114**, 198301 (2015).
[36] A. P. Solon, J. Stenhammar, M. E. Cates, Y. Kafri, and J. Tailleur, Phys. Rev. E **97**, 020602(R) (2018).
[37] T. Vicsek, A. Czirok, E. Ben-Jacob, I. Cohen, and O. Shochet, Phys. Rev. Lett. **75**, 1226 (1995).
[38] J. Elgeti, R. G. Winkler, and G. Gompper, Rep. Prog. Phys. **78**, 056601 (2015).
[39] E. W. Burkholder and J. F. Brady, J. Chem. Phys. **150**, 184901 (2019).
[40] G. Junot, G. Briand, R. Ledesma-Alonso, and O. Dauchot, Phys. Rev. Lett. **119**, 028002 (2017).
[41] J. U. Klamser, S. Kapfer, and W. Krauth, J. Chem. Phys. **150**, 144113 (2019).
[42] N. Nikola, A. P. Solon, Y. Kafri, M. Kardar, J. Tailleur, and R. Voituriez, Phys. Rev. Lett. **117**, 098001 (2016).
[43] H. Wang, T. Qian, and X. Xu, Soft Matter **17**, 3634 (2021).
[44] S. Dal Cengio, D. Levis, I. Paganobarraga, J. Stat. Mech. (2021) 043201.
[45] H. G. Wood and J. A. Hanna, Soft Matter **17**, 3137 (2021).
[46] C. Reichhardt and C. J. O. Reichhardt, Phys. Rev. E **103**, 022602 (2021).
[47] J. Denk and E. Frey, Proc. Natl. Acad. Sci. **117**, 31623 (2020).
[48] P. Herrera and M. Sandoval, Phys. Rev. E **103**, 012601 (2021).
[49] D. Dattler, G. Fuks, J. Heiser, E. Moulin, A. Perrot, X. Yao, and N. Giuseppone, Chem. Rev. **120**, 310 (2020).
[50] P. Liu, H. Zhu, Y. Zeng, G. Du, L. Ning, D. Wang, K. Chen, Y. Lu, N. Zheng, F. Ye, and M. Yang, Proc. Natl. Acad. Sci. **117**, 11901 (2020).
[51] L. Berthier, E. Flenner, and G. Szamel, J. Chem. Phys. **150**, 200901 (2019).
[52] G. Szamel, Europhys. Lett. **117**, 50010 (2017).
[53] G. Szamel and E. Flenner, Europhys. Lett. **133**, 60002 (2021).
[54] G. Szamel, Phys. Rev. E **90**, 012111 (2014).
[55] E. Flenner, G. Szamel, and L. Berthier, Soft Matter **12**, 7136 (2016).
[56] E. Flenner and G. Szamel, Phys. Rev. E **102**, 022607 (2020).
[57] L. Berthier, E. Flenner, and G. Szamel, New J. Phys. **19**, 125006 (2017).
[58] P. Karageorgiev, D. Neher, B. Schulz, B. Stiller, U. Pietsch, M. Giersig, and L. Brehmer, Nat. Mater. **4**, 699 (2005).
[59] G. J. Fang, J. E. Maclennan, Y. Yi, M. A. Glaser, M. Farrow, E. Korblova, D. M. Walba, T. E. Furtak, and N. A. Clark, Nat. Commun. **4**, 1521 (2013).
[60] N. Hurduc, B. C. Donose, A. Macovei, C. Paius, C. Ibanescu, D. Scutaru, M. Hamel, N. Branza-Nichita, and L. Rocha, Soft Matter **10**, 4640 (2014).
[61] J. Vapaavuori, A. Laventure, C. G. Bazuin, O. Lebel, and C. Pellerin, J. Am. Chem. Soc. **137**, 13510 (2015).
[62] V. Teboul, R. Barille, P. Tajalli, S. Ahmadi-Kandjani, H. Tajalli, S. Zielinska, and E. Ortyl, Soft Matter **11**, 6444 (2015).
[63] V. Teboul, M. Saiddine, J. M. Nunzi, and J. B. Accary, J. Chem. Phys. **134**, 114517 (2011).
[64] V. Teboul, M. Saiddine, and J. M. Nunzi, Phys. Rev. Lett. **103**, 265701 (2009).
[65] F. Mercier, G. Delhaye, and V. Teboul, J. Mol. Liq. **360**, 119545 (2022).
[66] J. B. Accary and V. Teboul, J. Chem. Phys. **139**, 034501 (2013).
[67] A. Natansohn and P. Rochon, Chem. Rev. **102**, 4139 (2002).
[68] J. A. Delaire and K. Nakatani, Chem. Rev. **100**, 1817 (2000).
[69] G. S. Kumar and D. C. Neckers, Chem. Rev. **89**, 1915 (1989).
[70] K. G. Yager and C. J. Barrett, Curr. Opin. Solid State Mater. Sci. **5**, 487 (2001).
[71] T. G. Pedersen and P. M. Johansen, Phys. Rev. Lett. **79**, 2470 (1997).
[72] T. G. Pedersen, P. M. Johansen, N. C. R. Holme, P. S. Ramanujam, and S. Hvilsted, Phys. Rev. Lett. **80**, 89 (1998).
[73] J. Kumar, L. Li, X. L. Jiang, D. Y. Kim, T. S. Lee, and S. Tripathy, Appl. Phys. Lett. **72**, 2096 (1998).
[74] C. J. Barrett, P. L. Rochon, and A. L. Natansohn, J. Chem. Phys. **109**, 1505 (1998).
[75] C. J. Barrett, A. L. Natansohn, and P. L. Rochon, J. Phys. Chem. **100**, 8836 (1996).
[76] P. Lefin, C. Fiorini, and J. M. Nunzi, Pure Appl. Opt. **7**, 71 (1998).
[77] D. Chandler and J. P. Garrahan, Annu. Rev. Phys. Chem. **61**, 191 (2010).
[78] M. P. Allen and D. J. Tildesley, *Computer Simulation of Liquids* (Oxford University Press, New York, 1990).
[79] M. Griebel, S. Knapek, and G. Zumbusch, *Numerical Simulation in Molecular Dynamics* (Springer-Verlag, Berlin, 2007).
[80] D. Frenkel and B. Smit, *Understanding Molecular Simulation* (Academic Press, San Diego, 1996).
[81] M. Pozar *et al.*, J. Chem. Phys. **145**, 144502 (2016).

[82] V. Teboul and J. B. Accary, Phys. Rev. E **89**, 012303 (2014).
[83] V. Teboul, J. B. Accary, and M. Chrysos, Phys. Rev. E **87**, 032309 (2013).
[84] S. Ciobotarescu, N. Hurduc, and V. Teboul, Phys. Chem. Chem. Phys. **18**, 14654 (2016).
[85] M. Saiddine, V. Teboul, and J. M. Nunzi, J. Chem. Phys. **133**, 044902 (2010).
[86] A. P. Kerasidou, Y. Mauboussin, and V. Teboul, Chem. Phys. **450-451**, 91 (2015).
[87] H. J. C. Berendsen, J. P. M. Postma, W. Van Gunsteren, A. DiNola, and J. R. Haak, J. Chem. Phys. **81**, 3684 (1984).
[88] R. J. Good and C. J. Hope, J. Chem. Phys. **53**, 540 (1970).
[89] J. Delhommelle and P. Millie, Mol. Phys. **99**, 619 (2001).
[90] L. Berthier, G. Biroli, J. P. Bouchaud, L. Cipelletti, and W. Van Saarloos, *Dynamical Heterogeneities in Glasses, Colloids and Granular Media* (Oxford Science Publications, Oxford, 2011).
[91] G. Biroli, P. Charbonneau, G. Folena, Y. Hu, and F. Zamponi, Phys. Rev. Lett. **128**, 175501 (2022).
[92] H. Ding, H. Jiang, and Z. Hou, Phys. Rev. E **95**, 052608 (2017).
[93] M. Bley, P. I. Hurtado, J. Dzubiella, and A. Moncho-Jorda, Soft Matter **18**, 397 (2022).
[94] In this paper we call respectively "above or below the transition" the medium that has undergone the phase transition or not. The reason is that our main parameter τ_μ is larger after the transition than before. Thus "above" or "below" refer to that critical parameter $\tau_\mu = \tau_\mu^c$.
[95] V. Teboul, in preparation.
[96] D. Chandler, *Introduction to Modern Statistical Mechanics* (Oxford University Press, New York, 1987).
[97] R. K. Pathria and P. D. Beale, *Statistical Mechanics*, (Academic Press, Oxford, 2011).
[98] H. Gould and J. Tobochnik, *Statistical and Thermal Physics* (Princeton University Press, Princeton, 2010).
[99] T. Speck, J. Stat. Mech. (2019) 084015.
[100] C. K. Mishra, K. H. Nagamanasa, R. Ganapathy, A. K. Soodb, and S. Gokhale, Proc. Natl. Acad. Sci. **111**, 15362 (2014).
[101] Y. S. Elmatad and A. S. Keys, Phys. Rev. E **85**, 061502 (2012).
[102] A. S. Keys, J. P. Garrahan, and D. Chandler, Proc. Natl. Acad. Sci. **110**, 4482 (2013).
[103] M. Isobe, A. S. Keys, D. Chandler, and J. P. Garrahan, Phys. Rev. Lett. **117**, 145701 (2016).